Curaua Leaf Fiber (*Ananas comosus* var. *erectifolius*) Reinforcing Poly(lactic acid) Biocomposites: Formulation and Performance

Marco Antonio Moreira de Araujo,[1] Alfredo Rodrigues de Sena Neto,[1] Elias Hage Jr.,[1] Luiz Henrique Capparelli Mattoso,[2] José Manoel Marconcini[2]
[1]*PPG-CEM/UFSCar, Rodovia Washington Luiz, Sao Carlos, Sao Paulo, Brazil*

[2]*National Nanotechnology Laboratory for Agrobusiness (LNNA), Embrapa Instrumentation, Rua XV de Novembro, Sao Carlos, Sao Paulo, Brazil*

Formulations of poly(lactic acid) (PLA) reinforced by curaua leaf fibers were prepared and characterized. This biocomposite has material characteristics such as biodegradability and renewability. This work aimed to develop a PLA/curaua leaf fiber composite as a sustainable biodegradable polymer composite. The PLA and composites were thermally, mechanically, and morphologically evaluated. The critical fiber length was studied to check its influence on the mechanical properties. Predictions of the Young's modulus were done to compare with the experimental data, having a reasonable agreement. The Young's modulus increased above 70%, and the impact strength increased 20% compared with the pure PLA. Thermal analysis showed that formulations with up to 20% by weight of fibers were more thermally stable. The fiber modified the crystallinity of the PLA matrix. The best overall balance of properties was attained in composites containing 15% curaua fiber. POLYM. COMPOS., 36:1520–1530, 2015.

INTRODUCTION

Biodegradable polymers were introduced in the 1980s and became commercially available in the 1990s. Biodegradable resins are still technologically and economically lagging behind conventional polymeric resins, which have been studied and developed over a much longer time period [1, 2]. This helps explain the challenges in terms of cost, manufacturing, and technical performance in commercializing biopolymers.

Those are the main barriers against their market participation (still about 10%), despite the rapid ascension. In that way, there is need of further development of biopolymers as matrixes in sustainable composites within an environmentally friendly concept [2]. Biocomposites have been increasingly emerging as alternatives to reduce the effects caused by the growing human activities and consumption [1–6].

Biodegradable polymers are mainly used for packaging, agriculture, medicine, and automotive applications. As mentioned, some of the biodegradable polymers engineering properties in their neat form may not be satisfactory or equivalent to those offered by conventional polymers, thus limiting the performance in many cases [1]. An opportunity to improve biodegradable resins is to reinforce them by vegetable fibers, as shown by several studies [4, 7, 8].

Biodegradable composites can be compared with glass fiber-reinforced composites [1]. Several advantages can be obtained by using natural fibers in biocomposites, in comparison with glass fibers or other inorganic fillers composites, such as, low cost, lower density, high mechanical strength, and less equipment wear. In addition, other positive characteristics are important, such as, biodegradability, recyclability, less skin irritation, or respiratory diseases by their handling. On the other hand, there are some limitations, such as, high moisture absorption, which may depress mechanical properties, occasional poor compatibility with hydrophobic polymeric resins, low processing maximum working temperature, and seasonality for crops [5, 6, 9–13]. Despite those limitations, lignocellulosic fibers are emerging as reinforcement alternatives in polymer matrices composites for a wide variety of applications.

The poly(lactic acid) (PLA), used in the present work as biodegradable matrix, is a material with interesting characteristics, such as biocompatibility and bioabsorptivity, attracting environmental and biomedical interest. PLA has high mechanical strength compared with thermoplastic resins, as well as some similar properties in comparison with resins such as polyethylene terephthalate and PP

Correspondence to: Mr. Alfredo Rodrigues de Sena Neto; e-mail: alfredosena@yahoo.com.br
DOI 10.1002/pc.23059
Published online in Wiley Online Library (wileyonlinelibrary.com).

TABLE 1. Compositions of different vegetable fibers [23].

Composition (%)	Coir	Jute	Ramie	Sisal	Curaua
Cellulose	43.4–53	60	80–85	60–75.2	70.7–73.6
Hemicellulose	14.7	22.1	3–4	10–15	21.1
Lignin	38.3–40.77	15.9	0.5	8–12	7.5–11.1
Ashes	–	1	–	0.14–0.87	0.79–0.9

[14]. A variety of studies have been conducted using PLA as matrix in composites with cellulosic fibers [15–18].

The incorporation of fibrous reinforcement in the PLA does not always improve tensile strength in injection-molded materials. Ibrahim et al. [19], by incorporating kenaf fibers into PLA matrix and using triacetin plasticizer, reduced the depreciation in PLA's tensile strength and increased elongation at break. Lee and Wang [20] studied the use of lysine diisocyanate with similar purpose in a PLA matrix reinforced by short bamboo fibers without, however, achieving any improvements upon the neat PLA. Jandas et al. [21] analyzed the effects of banana fibers in PLA composites, also observing decrease in tensile strength and elongation at break. Impact strength had also been lowered compared with the matrix material. Only fibers treated on NaOH solution followed by adding bis-(3-triethoxy silyl propyl) tetrasulfane led to composites with superior impact properties, although with inferior tensile strength and elongation values. Oksman et al. [22] found that extruded and thermopressed PLA–flax fibers (30% mass fraction) composites showed tensile strength equivalent to that of neat PLA, whereas having higher Young's modulus and lower impact strength and elongation. Table 1 [23] shows chemical compositions and some physical and chemical characteristics of different vegetable fibers.

In this work, the fibers used in the composites were extracted from curaua (*Ananas comosus* var. *erectifolius*) leaves. Studies on that fiber are recent, with rapidly growing interest in the last decades. The curaua fibers' high tensile strength and Young's modulus are equivalent to some advanced synthetic fibers, as observed in Table 2 [23, 24], and have called attention for industrial engineering applications, mostly as thermoplastic composites [5, 25–27]. Regarding the use of curaua fibers in PLA composites, few works in the literature focus on analyzing the effects of its incorporation in composites with PLA. The curaua fiber is a promising lignocellulosic leaf fiber. It has a suitable combination of properties with the same cost as other lignocellulosic fibers, many of which have lower tension and flexural strength properties such as coir, sisal, or jute.

Curaua-based composites also perform better than other natural fiber/polypropylene (PP) composites, widely used in the automotive industry [5, 28]. Castro et al. [29] prepared composites with high-density biopolyethylene and curaua fibers either by premixing and thermopressing, or by extruding and then injection molding. Hydroxyl-terminated polybutadiene was used as the compatibilizing agent. It was seen that the curaua fibers enhanced properties such as flexural strength, storage modulus, and impact strength of high-density biopolyethylene, aided by the adhesion provided by the hydroxyl-terminated polybutadiene. The fiber dispersion, flexural strength, and impact strength were observed to be higher in the extruded and injection-molded composites. Harnnecker et al. [30] studied composites of Ecovio® and curaua fibers, with and without maleic anhydride grafted PP (MA-*g*-PP). The composites without MA-*g*-PP had lower tensile strength compared with neat Ecovio, with a maximum for the 15 wt% formulation. Young's modulus was higher for all the formulations, increasing with the fiber fraction. Composites with MA-*g*-PP showed superior tensile strength and modulus, compared with the neat Ecovio and composites without the agent with same fiber contents. The best overall properties were seen for the 15 wt% curaua formulations. Pure Ecovio did not break under impact at the given conditions. The composites broke, having more fragile behavior with larger fiber contents. The composites had higher flexural strength and modulus, increasing with the fiber curaua fraction. Borsoi et al. [31] evaluated properties of virgin or recycled extruded/injected polystyrene in composites with 20 wt% of curaua fibers. The addition of fibers led to an increase in the tensile strength, modulus of elasticity, rigidity, thermal stability, and melt viscosity. Pullouts were observed by microscopy because of the poor adhesion between fiber and reinforcement. The impact strength was observed to be lower with the presence of the fibers. Borsoi et al. [32] also researched recycled expanded polystyrene (EPS)–curaua composites through photo and biodegradation. The composites showed higher modulus and tensile strength compared with the resin. The mechanical properties were also higher under composting and ultraviolet aging.

Given the interesting properties of both PLA and curaua fibers for use in composites, this work aims to characterize a novel extruded/injection-molded composite

TABLE 2. Physical and mechanical properties of vegetable and synthetic fibers.

Fiber	Tensile strength (MPa)	Young's modulus (GPa)	Reference
Cotton	400	12	[23]
Jute	400–800	10–30	[23]
Ramie	500–870	44	[23]
Sisal	324–630	17–22	[23]
Curaua	1,250–3,000	30–80	[23]
Aluminum oxide	1,380	379	[24]
Aramide (Kevlar 49)	3,600–4,100	131	[24]
Carbon	1,500–4,800	228–724	[24]
E-glass	3,450	72.5	[24]
Boron	3,600	400	[24]
Silicon carbide	3,900	400	[24]
UHMWPE (Spectra 900)	2,600	117	[24]

of PLA matrix reinforced with curaua leaf fibers. The study compares theoretical (calculated) mechanical properties with those obtained experimentally.

EXPERIMENTAL

Materials

The mechanically separated curaua (*Ananas comosus* var. *erectifolius*) leaf fibers bundles were kindly provided by Pematec (Santarem, PA, Brazil). The fibers were not subjected to any chemical or surface treatment to avoid any cumulative or harmful substances to the environment. The overall average diameter of the fiber cell bundles was measured using a digital metallic micrometer caliper. The values were used in the tensile strength and Young's modulus calculations of the nonincorporated fibers. The diameter of fiber cell bundles is within the expected range: 64.2 ± 16 μm, and the individual values ranged from 36 to 101 μm. Spinace et al. [33] obtained an average diameter value of 60 μm. The material used in the matrix was an injection-grade PLA Ingeo 3251D, with specific gravity of 1.24 g/cm^3 and MFI (melt flow index) of 35 g/10 min (at 190°C and 2.16 kg); provided by Nature Works LLC [34].

Methodology

For the reinforcement preparation, the fibers bundles were chopped in a KIE MAK 250 knife mill, sieved in 18 mesh for the removal of the largest possible quantity of fibers with less than 1 mm in length, and finally incorporated to the PLA.

For better understanding of behaviors of the melted PLA and composites, planning of the processing variables and selection of the most appropriate percentages of reinforcement for the formulations during extrusion, an analysis was realized using a HAAKE Rheomix 600 internal mixer connected to a torque rheometer. The mixing torque was registered with the time up to 7 min for all compositions. Both PLA and curaua fiber bundles were previously weighed and then poured in the internal mixer chamber, heated at 185°C, at once with the counter-rotating blender rotors running at 50 rpm. The mass of fibers varied between 10% and 70%, with 10% increments. The aim was to get formulations with largest possible fiber content that could be processed in standard equipments for thermoplastics; in this case, extruder and injection-molding machine.

Six composite formulations (5%, 10%, 15%, 20%, 30%, and 40% fibers by weight) and neat PLA were processed in a twin-screw Coperion ZSK 18 extruder, with gravimetric feed. The screw profile is composed of three kneading and two left hand mixing zones, as well as one left hand conveying element. The heating zones had the following temperature profile from Zone 1 to Zone 7, respectively: 140°C, 150°C, 160°C, 160°C, 170°C, 180°C, and 190°C. The screw speed was 300 rpm for neat PLA, 5%, 10%, 15%, and 20% curaua formulations. For 30% and 40% formulations the speed was 500 rpm. Tensile test specimens were injection molded with use of an Arburg Allrounder 270 S injection-molding machine. The temperature profile from Zone 1 to Zone 5 was, respectively, 115°C, 170°C, 190°C, 200°C, and 205°C. The specimens were submitted to tensile tests with five repetitions per material, following ASTM D638 standard Type 1. The equipment used was an Emic DL3000 universal testing machine, with 5 mm min^{-1} crosshead speed. The tensile properties of fiber bundles were measured in accordance with ASTM D3379 standard adaptation, with 30 repetitions. The fiber bundles cross-section were considered solid and bulky, as free of voids, for the calculations.

Notched Izod impact tests were performed in all seven material varieties, following ASTM D256 standard. The equipment used was a Tinius Olsen model Impact 104. Ten samples were tested for each formulation.

A thermogravimetric analyzer TA Instruments model T500 was used in the thermal analysis of pure PLA and the composites. Each sample was cut from tensile test specimens, and undergone a 10°C min^{-1} heating rate, from room temperature to 600°C in synthetic air atmosphere (20% O_2 + 80% N_2). One sample of curaua fibers was analyzed under same conditions.

The influence of the fibers on the matrix crystallinity was studied through differential scanning calorimetry with a TA Instruments calorimeter model Q100 in heat flux mode. The specimens were used as taken from injection-molded specimens. The heating rate was 10°C min^{-1}. The initial equilibrium temperature was 40°C. The samples were then heated to 210°C followed by cooling to −80°C, followed by other heating cycle to 210°C. The nitrogen flux was set to 60 ml min^{-1}. The crystallinity indexes were calculated according to *Eq. 1*:

$$\%X_C = \{[\Delta H_1 - (\Delta H_2 + \Delta H_3)]/(\Delta H_0)\} \times 100 \qquad (1)$$

ΔH_1 is the enthalpy referring to the first heating cycle fusion peak. ΔH_2 and ΔH_3 are the enthalpies of the first and second crystallization peaks, respectively, also in the first heating cycle. Finally, ΔH_0 corresponds to the theoretical 100% crystalline PLA enthalpy, whose value is 93.7 J g^{-1} for the poly(L-lactic acid) [35]. The aim was to analyze each formulation, comparing the curves with and without thermal history. The mass fractions of the fibers in the formulations were discounted. The values collected are related to the first cycle.

For the morphological analysis, the injection-molded samples were cryofractured and observed by scanning electron microscopy (SEM), using a JEOL JSM 6510 with accelerating voltage of 15 kV. The average fiber lengths (l_f) and diameters (d_f) of cell units inside the composites were necessary for the micromechanics calculations. The measurement was done using films prepared

 DOI 10.1002/pc

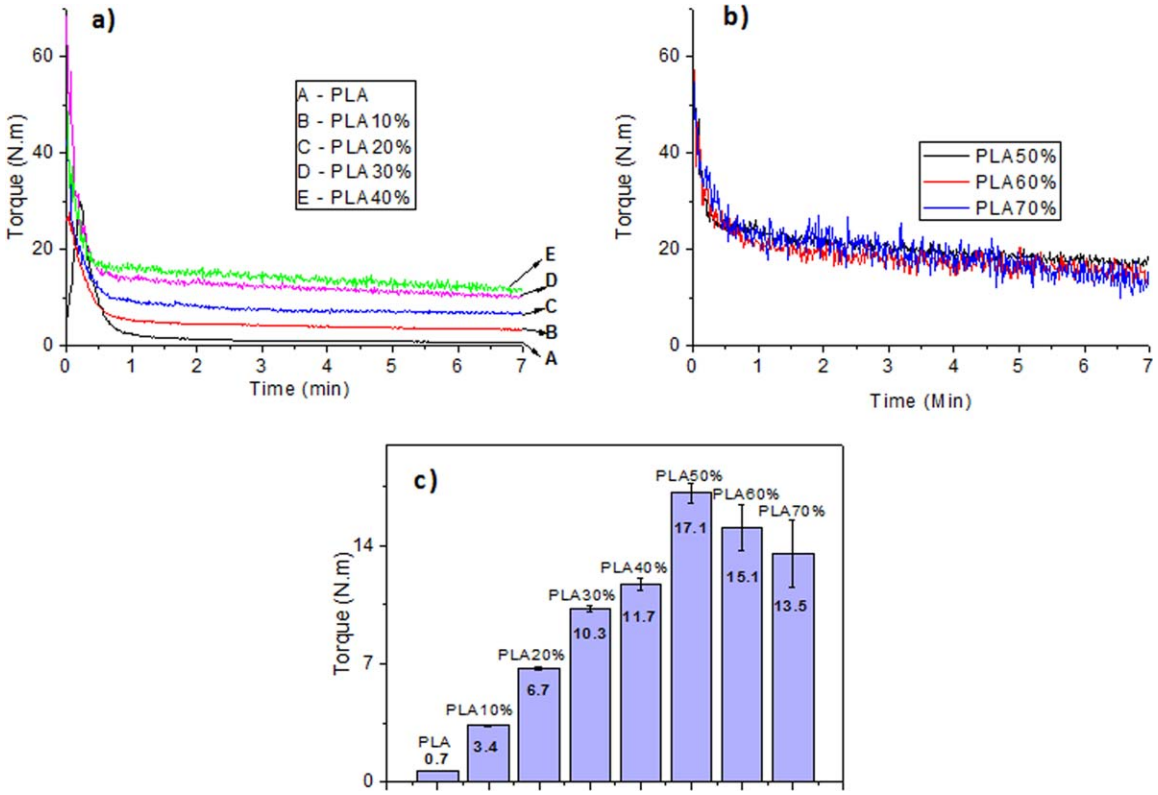

FIG. 1. Torque evolution for (a) pure PLA and composites with 0% to 40% w/w of fibers and (b) for the mixtures with 50%–70% w/w of fiber and the pure-fiber mass, in 7 min of test at 185°C. (c) Average torque for the range of 6.5–7.0 min of test. [Color figure can be viewed in the online issue, which is available at wileyonlinelibrary.com.]

from the solubilized injected specimens using chloroform. The solutions were deposited and dried on glass slides. The films were observed with a polarized light optical microscope Leica model DMRXP at ×100, ×200, and ×400 magnifications. The measurements were done with aid of the software Image J 1.46. The chloroform did not cause significant swelling to the fibers.

RESULTS AND DISCUSSION

PLA/Curaua Fiber Composite: Preliminary Compounding in an Internal Mixer

Figure 1 shows the melt compounding behavior for the PLA/curaua fiber composite prepared in an internal mixer. After reaching a torque peak, as a result of the solid materials fed in the internal mixer chamber at room temperature, all the compositions had their torque values decreased and level off within the time less than 2 min due to the melt mixing process. As the curaua fiber content is increased up to 40% w/w the torque values level off at higher values, as observed in Fig. 1a. For higher amounts of curaua fibers in the composites, the torque values have followed the same trend; however, for fiber contents between 50% and 70% w/w, the torque curves kept in the same level, as observed in Fig. 1b. In addition, it can be noticed that the torque curves were not as smooth as observed in Fig. 1a due to the presence of larger amounts of curaua fibers, which have been kept as solid major phase during mixing. This behavior has indicated that the fiber fractions greater than 40% w/w may decrease the fibers mixing and wetting by the polymer, preventing the processing in many traditional processing equipments such as extruders and injection-molding machines. Figure 1c shows the average torque curve in the mixing time range of 6.5–7 min, for pure PLA and PLA with concentrations from 10% up to 70% of curaua fibers by weight. As can be seen in the bar graphs, the torque data reaches a maximum in the formulation with 50% w/w of curaua fiber. For that fiber concentration (50% w/w) and above the torque magnitude was considered deleterious to the fibers, possibly leading to their break or degradation while processing in conventional extruders. The increased torque would also lead to higher shear and pressure in the extruder and in the injection-molding machine, which again may lead to degradation and to an ineffective dispersion of the reinforcement. Viscous heating and fiber–fiber friction led to temperature increases up to 18°C from the nominal 185°C. Considering all those results, formulations with 5%, 10%, 15%, 20%, 30%, and 40% by weight of curaua fiber were chosen to be extruded and mold injected.

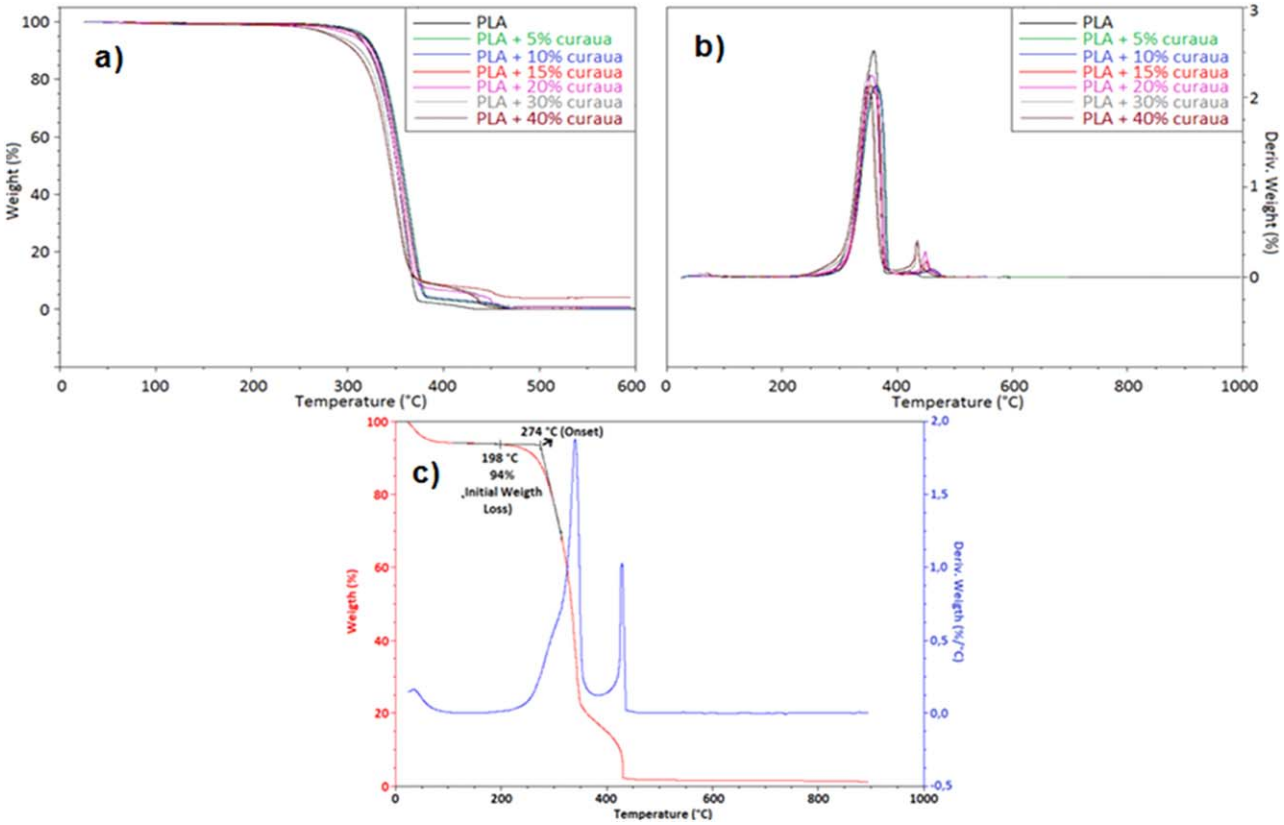

FIG. 2. TGA (a) and differential thermogravimetric (b) curves of the PLA matrix and the six composite formulations. (c) TGA and differential thermogravimetric curves of curaua leaf fiber bundles. [Color figure can be viewed in the online issue, which is available at wileyonlinelibrary.com.]

PLA/Curaua Fiber Composites Thermal Behavior

Thermogravimetry. Figure 2 presents the pure PLA, its composites, and the curaua fiber's respective weight loss and derivative curves obtained by thermogravimetric analysis (TGA). The curves (Fig. 2a and b) show similar behavior for all formulations, with small variations between the decomposition temperatures. It is seen that the composites with higher fiber content present a second thermal decomposition stage at 350°C–450°C due to the fiber's lignin thermal degradation. A second peak at differential thermogravimetric curve, as shown in Fig. 2c, may confirm the degradation of the lignin component from the fiber. In addition, it can be noticed from Fig. 2c a loss of approximately 6% w/w of water from the curaua fiber. The first main stage of mass loss is related to the PLA, cellulose, and hemicellulose decompositions. The initial weight loss temperature by thermoxidative degradation can be located on the TGA curves as the first point where a nonlinear mass decay happens as the temperature increases. The onset temperature is seen in the central section as a "shoulder-like" part of the mass loss TGA curves. Both temperatures are indicated in Fig. 2c. The corresponding temperatures of each occurred thermal event are shown in Table 3.

The initial weight loss and onset temperatures have not decreased as the fiber mass fractions ranged from 5% to 20% w/w, showing a stable thermal interaction between the composites components. Those temperatures were superior to the pure PLA value. The thermal stability was found to decrease in the composites with 30% and 40% of curaua fibers. The composites were extruded and processed in temperatures lower than the lowest observed for initial thermoxidative weight loss temperature.

Differential Scanning Calorimetry. Figure 3 shows the heating and cooling cycles from the DSC, pointing the first and second heating cycles, as well as the transitions occurred within each peak of the curves. Table 4 contains the temperatures and enthalpies of the main points of the DSC curves, and the crystallinity index for PLA and formulations. According to Fig. 3 and Table 4, all formulations have shown great similarity in the DSC curves shape and in the transition temperatures during the heating cycles. This is in agreement with the fact that all the thermal transitions are attributed to the PLA only. As it was shown in the curaua fibers TGA, they have not undergone to thermal transitions at temperatures lower than 210°C. Nevertheless, the enthalpy values have changed, most of the time increasing, by adding curaua fibers, which may indicate that curaua fibers prevent the rearrangements of the PLA molecules. The shift between

 DOI 10.1002/pc

TABLE 3. Samples thermal transition temperatures.

Formulation	Initial weight loss temperature by thermoxidation (°C)	Onset temperature (°C)
PLA	260	326
P5%C	268	333
P10%C	263	332
P15%C	254	330
P20%C	250	328
P30%C	244	325

curves, corresponding to the first and the second cycle in the range of 40°C–210°C, may indicate changes occasioned by the materials thermal history. The slight decrease in heat flow between 59°C and 64°C may be due to rearrangement of the molecules in the amorphous portion of rigid amorphous phase in PLA [36, 37].

The highest value of crystallinity index was composite containing 5%, followed by a downward trend in the value of the crystallinity index with increasing fraction of curaua fibers. For fractions with 30% and 40%, the crystallinity index values are close to the pure matrix. The curaua fibers act like nucleating agent, but larger fractions of curaua fibers difficult becomes the crystal ordering of the PLA molecules. This may be a possible reason why the melting temperature slightly decreases when the curaua fiber contents become larger in the composites. The improvement in mechanical properties for some formulations compared with the others, as will be shown later, can be explained by that crystallinity effects and the mechanical reinforcement due to the presence of the fibers. Also, it is relevant to point out that the composites mechanical properties come, among other factors, from the balance of the effects of both phases crystallinity. For the vegetable fibers used, the relatively high crystallinity of the cellulose contained in the curaua fibers and its gender (*Ananas*) characteristic structural organization, as well as the high content [38–41], caused the effective increments in Young's moduli (and less effective increments in the 30% and 40% w/w curaua composites).

PLA/Curaua Fiber Composite Microstructure Observed by SEM

Figure 4 shows composite micrographs taken from the cryofractured surfaces injection-molded specimens. The micrographs are indicating the occurrence of brittle fracture characteristics for all samples. The pure PLA apparently shows no voids, which may indicate the use of appropriate molding conditions.

The composites processing conditions and the fiber bundles wetting by the matrix were sufficient to filamentize the bundles of fibers as single fiber, which show high aspect ratio, larger cellulose content, and, in general, good reinforcing mechanical properties. The single fiber observed in the micrographs has an average diameter between 4 and 8 μm. Both reasonable fiber dispersion and distribution were evidenced in the composite samples. No contacts were observed between single fibers. The specimens cryofracturing was done in a transversal direction to the melt flow in the injection-mold cavity. As a consequence, a tendency of a perpendicular fiber orientation to the fracture plane was observed. The fibers have not received any surface or coupling treatment. As a consequence, there was no strong interfacial adhesion between the PLA and the single fiber. Presence of debonding around the fiber in the PLA matrix can be easily observed. The same interface characteristics have already been observed in the literature [15–18].

PLA/Curaua Fiber Composite Mechanical Properties

Figure 5 shows the tensile testing behavior for PLA and its composites with curaua fibers. PLA has shown a

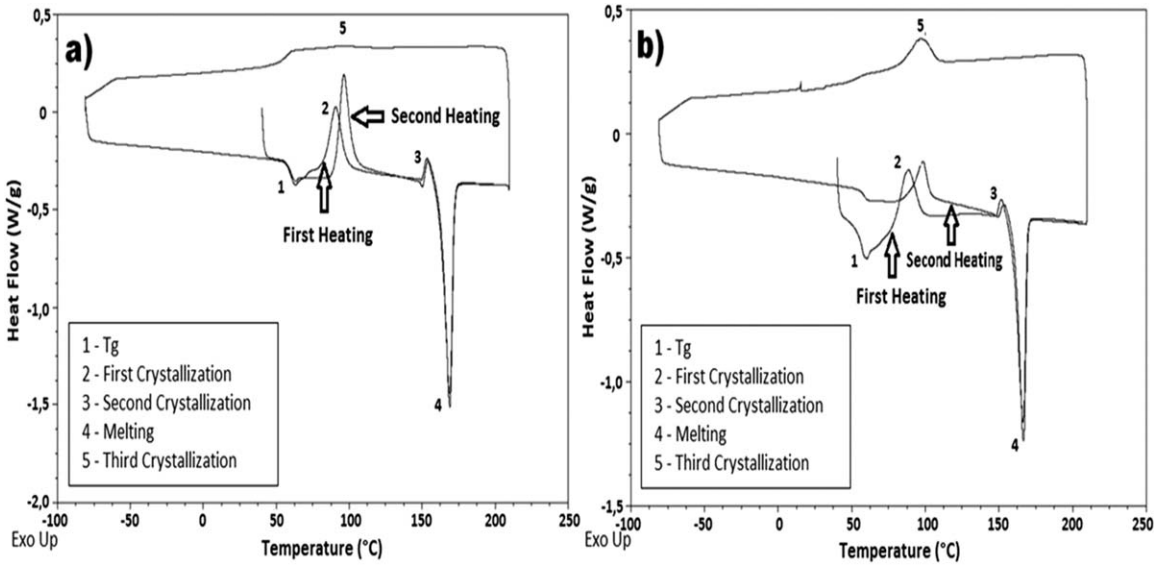

FIG. 3. DSC curve for (a) the pure PLA and (b) the 40% w/w curaua fiber content in the composite.

TABLE 4. Transition temperatures, the corresponding enthalpies, and the crystallinity indexes for all formulations during the first heating step.

		First crystallization (cold)		Second crystallization (cold)		Melting		Third crystallization (hot)		
Formulation	T_g (°C)	T_{C1} (°C)	ΔH_{1C} (J/g)	T_{C2} (°C)	ΔH_{2C} (J/g)	T_m (°C)	ΔH_m (J/g)	T_{C3} (°C)	ΔH_{3C} (J/g)	X_c (%)
PLA	59	91	19.3	153	2.6	169	43.1	96	1.0	22.6
P5%C	60	90	18.6	153	2.7	168	52.4	94	1.9	33.1
P10%C	58	88	18.8	153	2.4	169	48.2	92	2.7	28.8
P15%C	56	88	22.1	153	2.9	167	50.6	93	4.8	27.4
P20%C	57	88	19.9	153	2.9	167	49.8	94	4.2	28.9
P30%C	57	89	22.6	153	2.7	167	43.5	96	11.7	19.4
P40%C	56	88	28.7	152	2.5	166	52.7	96	16.2	23.0

well-defined yielding stress at the curve. PLA composites with 5% of fiber also showed similar curves to the PLA one. As the fiber content increased, most of the PLA composite curves have shown a more brittle behavior.

Table 5 shows the mechanical behavior data for the tensile testing and the Izod impact strength. Curaua fiber has significant Young's modulus and tensile breaking strength. Considering that the tensile properties were not measured on single fibers, but on bundle fibers, both modulus and strength are not far from the ones of some synthetic fibers, as shown in Table 2. The cellulose content in the curaua fibers (as shown in Table 1) and their fibrous structure may be the main reasons for their suitable mechanical properties. This was also shown in other studies on *Ananas* genus fibers [31].

The PLA tensile properties shown in Table 5 have confirmed what was observed by Henton et al. [14], as its modulus and strength are very close of some thermoplastics such as PP and polyethylene terephthalate. As curaua fibers are added to PLA, the composite modulus has shown an increase as should be expected. However, its tensile strength has not been improved compared with the

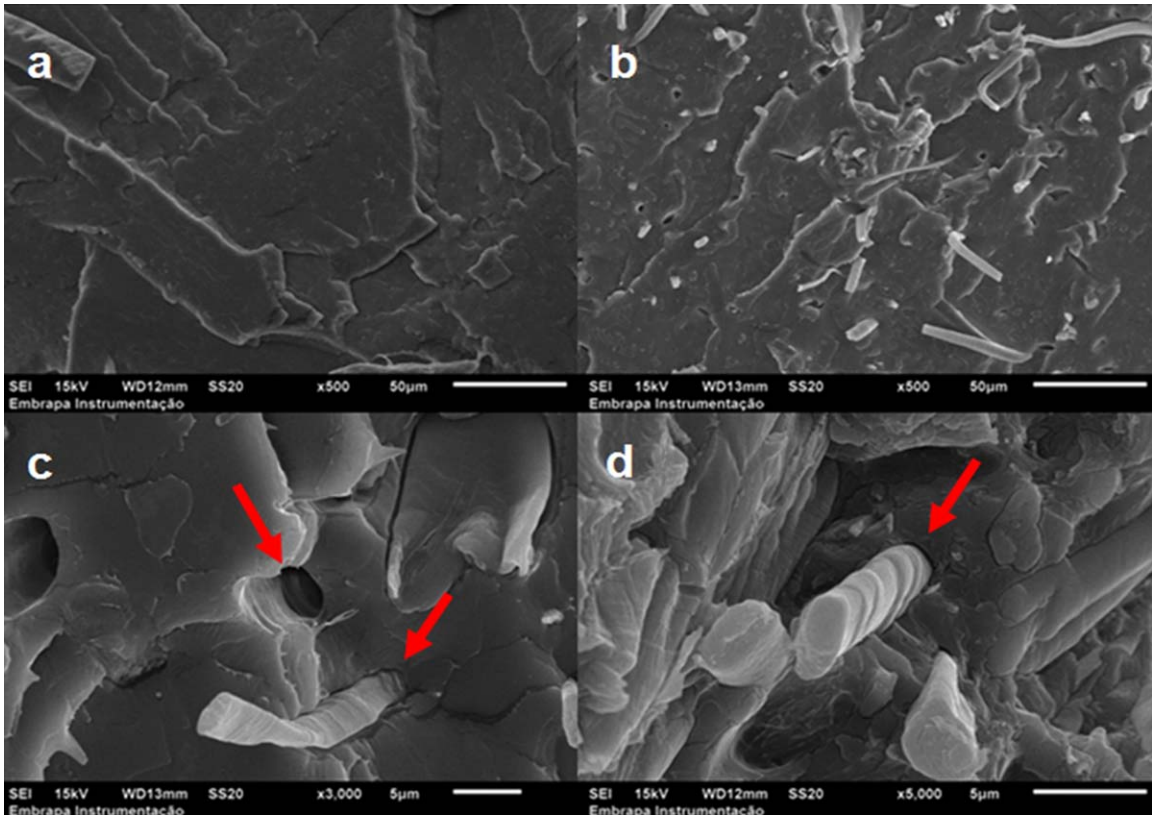

FIG. 4. Microstructures of the injection-molded samples by SEM: (a) pure PLA; (b) PLA5%C (×500 magnification); (c) PLA5%C (×3,000 magnification); and (d) PLA40%C (×5,000 magnification). Arrows indicate curaua fiber pullout or lack of interface adhesion. [Color figure can be viewed in the online issue, which is available at wileyonlinelibrary.com.]

 DOI 10.1002/pc

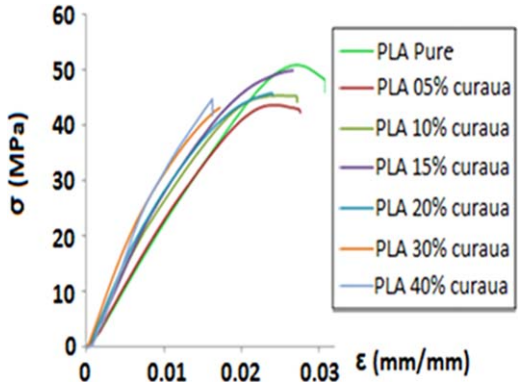

FIG. 5. Tensile stress–strain curves of the neat PLA and its composites with PLA/curaua. [Color figure can be viewed in the online issue, which is available at wileyonlinelibrary.com.]

neat PLA. The tensile strength of the PLA and its composites ranged between 40 and 52 MPa, which is superior to PP/flax fibers, a composite widely used in the automotive industry, and comparable with PLA/flax, as seen in other results of the literature [22]. No significant changes have been observed in the composites breaking strain containing up to 20% of curaua fibers. For higher fiber contents, a decrease in the breaking strain was observed, may be due to voids formation in the composite matrix.

The presence of presence of curaua fibers has improved the notched composites impact strength, increasing the propagating crack's path before reach the fracture and dissipating energy through the fibers break or pull out [42, 43]. The addition of fibers in PLA up to 20% w/w content improves the material impact strength. The P30%C and P40%C composites had much higher concentrations of voids and pulled out fibers, increasing the concentration of microscopic cracks, resulting in lower properties. Huda et al. [15] obtained composites with lower impact strength compared with the neat PLA matrix, even with the use of coupling agents. Bax and Müssig [18] also obtained PLA–flax composites with inferior impact properties compared with the PLA; however, improvements were observed for higher fiber contents. The composites tested with cordenka fibers showed superior impact strength, surpassing neat PLA. Bledzki et al. [16] achieved increments in impact strength of PLA composites both with abaca and cellulose fibers, through the use of an alternative extrusion/coating process and thus maintaining up to 15 mm long fibers, which was limited only by the pelletizing steps. Longer fibers absorb more impact energy, as the crack propagates through a greater distance with the presence of the same.

The effects of the curaua fiber in the composites are somewhat similar to other works using different vegetable fibers and fiber treatments. Huda et al. [15], also studying the mechanical behavior of lignocellulosic reinforced PLA composites without coupling treatments or surface fiber modifications, obtained 20%, 30%, and 40% w/w vacuum-dried wood-fiber/PLA composites prepared by extrusion and injection molding. The results showed that the presence of the fibers limited the polymer matrix deformation, and increased the composite modulus up to 133%. However, the moduli were inferior to the calculated values, and the tensile strength of the composites have not shown significant improvement over the PLA and decreased in comparison for the 40% w/w fibers composite, due to inadequate wetting and lack of interfacial compatibility. Similarly, Bledzki et al. [16] obtained biocomposites in PLA matrix without use of coupling/surface treatments, comparing the effects of reinforcement with man-made cellulose and abaca fibers. The abovementioned limitations regarding lack of compatibility were partially suppressed with the use of a preprocessing coating step during extrusion through a coating wire die and by incorporation of long fibers in the PLA. Even though the obtained pellets were subsequently further extruded and pelletized a second time for posterior injection molding, the tensile strength and moduli of the composites with 30% w/w fibers increased by a factor of 1.45 and 1.70, respectively, with man-made cellulose fibers, and by a factor of 1.20 and 1.40 with abaca fibers, respectively.

Many studies have been made by using fiber treatments to improve adhesion between the lignocellulosic fibers to the polymeric matrix. Cunha et al. [17] have shown the difference between distinct methods of fiber treatment prior to their incorporation in a PLA matrix, for spent cellulose and pine wood to be applied in the automotive industry. The fibers were either washed in hot water, simultaneously delignified or acetosolve treated, besides be submitted to autohydrolysis and washed in

TABLE 5. Measured parameters and mechanical properties of the curaua fibers and the composites.

Mechanical properties	Young's modulus (GPa)	Tensile strength (MPa)	Breaking strain (mm/mm)	Notched Izod impact strength (J/m)
Neat PLA	2.4 ± 0.1	51.6 ± 1.5	0.029 ± 0.002	8.6 ± 1.00
Curaua fiber	54.2 ± 17.2	1415 ± 413.4	0.038 ± 0.052	–
P5%C	2.6 ± 0.1	43.0 ± 0.4	0.028 ± 0.002	10.0 ± 0.66
P10%C	2.9 ± 0.2	46.1 ± 1.0	0.027 ± 0.001	9.7 ± 1.51
P15%C	3.3 ± 0.1	49.3 ± 0.9	0.027 ± 0.002	10.3 ± 0.54
P20%C	3.6 ± 0.1	45.6 ± 0.9	0.023 ± 0.001	10.3 ± 1.33
P30%C	3.9 ± 0.3	40.8 ± 2.7	0.016 ± 0.002	7.6 ± 1.41
P40%C	4.1 ± 0.4	42.0 ± 3.5	0.017 ± 0.002	4.8 ± 0.65

TABLE 6. Volumetric fraction, l_c, and l_f values for each formulation.

Formulation	Calculated volumetric fraction (φ_f)[a]	Critical length (l_c)[b] (mm)	Measured average length (l_f) (mm)
P5%C	0.044	0.098	0.420 ± 0.217
P10%C	0.090	0.078	0.461 ± 0.236
P15%C	0.135	0.067	0.330 ± 0.185
P20%C	0.183	0.059	0.142 ± 0.084
P30%C	0.275	0.048	0.105 ± 0.069
P40%C	0.371	0.041	0.050 ± 0.026

[a]Calculated from *Eq. 6*.
[b]Calculated from *Eq. 5*.

alkaline solution or swelled in isopropanol/NaOH solution and submitted to carboxymethylation by derivatization via addition of monochloroacetic acid in the solution. The results showed that the washed fibers showed better results in the 20 wt% fiber composites overall. The tensile strength, however, has not been significantly improved and has decreased with the incorporation of autohydrolyzed fibers. The 30% w/w fiber composites had improved stiffness without the cost of other mechanical properties losses.

Despite the defects observed within the material in the present study and the lack of chemical compatibility between the components, three main factors can be pointed out based on the fibrous composites micromechanics that may have contributed to the Young's modulus and the impact strength improvement for some of the formulations:

1. The existence of mechanically anchored single fibers in the matrix;
2. A sufficient fiber length to efficiently transfer applied stresses from the matrix to the single fiber;
3. Good distribution and dispersion of the single fiber, within some formulations, that have led to efficient wetting of the fibers and larger available surface area to the contact with the polymer, which has improved the stress transfer from the PLA to the single fibers.

Because the fibers have an essentially elastic behavior and the polymer molecular chains rearrangements were restricted, larger fiber contents in the composite may led to smaller breaking strain. Also, the stress transfer to the single fibers has reduced the polymer molecules stretching. The correlation between elastic modulus and the curaua fiber content is in accordance to the composite materials theories [42, 43].

Theoretical Analysis and Comparison Methodology of Measured and Calculated Elastic Modulus

One analysis to be accomplished regarding the Young's modulus of the composites can be done through Halpin–Tsai *Eqs. 2* and *3*, which may consider longitudinally aligned short discontinuous fibers. That may be done despite considering ideal conditions, such as ideal adhesion between fiber and matrix and absence of defects throughout the composite, as considered by Agarwal et al. [42]. Halpin–Tsai equation establishes two limits for Young's modulus values: the higher limit (E_{cl}) assumes that the fibers are longitudinally positioned to the load-bearing axis; and the lower limit (E_{ct}) considers that all the fibers have are transversely oriented. Those limits help to estimate ideal values for situations with fully oriented fibers and thus a theoretically possible range of values for a specific composite.

The maximum and minimum limits for the Young's modulus (E_{cl}) may be obtained with *Eq. 2*:

$$E_{cl} = \left(\frac{1+\xi\eta\varphi_f}{1-\eta\varphi_f}\right)E_m \tag{2}$$

where φ_f is the fiber volume fraction contained in the composite, E_m is the matrix tensile modulus, ξ is a value that reproduces the composite's type of modulus considering the fibers geometry, arrangement, and direction relative to the load application axis. For E_{cl}, in this study, $\xi = 2(l_f/d_f)$, η is the relation between the modulus of the fiber and the matrix, given by *Eq. 3*:

$$\eta = \frac{\left(\frac{E_f}{E_m} - 1\right)}{\left(\frac{E_f}{E_m} + \xi\right)} \tag{3}$$

The lower Young's modulus limit E_{ct} or transversal modulus, considering the ideal conditions mentioned, can be also calculated by *Eq. 2*, where ξ in this condition, has the value of 2 [42, 43].

The theoretical value of the elastic modulus for short fiber composites without a preferential orientation (E_{random}) is given by *Eq. 4* and based on E_{cl} and E_{ct}

$$E_{random} = \frac{3}{8}E_{cl} + \frac{5}{8}E_{ct} \tag{4}$$

Composites micromechanics [42–44] predicts that reinforcing short fibers should have a minimum length, which allows an efficient stress transfer from the matrix to the short fibers. The minimum length that the fibers should have to be considered effective is related to a critical length, which can be calculated. According to Rosen [44], the minimum critical length or ineffective length of a discontinuous fiber (l_c) from which there is no free decoupling of the same from the matrix is defined by *Eq. 5*. Rosen has used φ as stress ratio as 0.9, which means that the effective length is that portion of the fiber in which the average axial stress is equal to 90% of the stress that a continuous fiber would bear. In other words, this means that a fiber length in which the transferred axial stresses are immediately lower than 90% of tensile strength of the same type continuous fiber is, for $\varphi = 0.9$, called ineffective length. The value of l_c is simply the transition between the length considered ineffective to the effective.

TABLE 7. Young's modulus obtained from theoretical calculations, using Halpin–Tsai equation, for different fiber orientations obtained experimentally.

	Elastic moduli (E) (GPa)			
	Calculated E (GPa)			
Formulation	Longitudinal (E_{cl})[a]	Transversal (E_{ct})[a]	Random (E_{random})[b]	Measured E_{random} (GPa)
P5%C	4.4	2.7	3.3	2.6
P10%C	6.5	3.0	4.3	2.9
P15%C	8.3	3.4	5.2	3.3
P20%C	9.0	3.8	5.7	3.6
P30%C	12.0	4.7	7.4	3.9
P40%C	12.7	5.9	8.4	4.1

[a]The moduli obtained from *Eq. 2* were taken from average values of fiber length and diameter experimentally measured by optical microscopy.
[b]E_{random} was obtained from *Eq. 4*.

One of Rosen's important considerations is that the volume ratio of fibers within the matrix influences l_c and is inversely proportional to it, as shown in *Eq. 5*.

$$l_c = \frac{d_f}{2}\left[\frac{\left(1-\phi_f^{1/2}\right)}{\phi_f^{1/2}}\left(\frac{E_f}{G_m}\right)\right]^{1/2} \cosh^{-1}\left[\frac{1+(1-\varphi)^2}{2(1-\varphi)}\right] \quad (5)$$

where d_f is the single fiber diameter, E_f is the fiber modulus, G_m is the matrix shear modulus, and ϕ_f is the fiber volume fraction.

Equation 5 has been applied to the PLA/curaua fibers composites, where d_f has been chosen as the average diameter of the fibers observed and measured by optical microscopy, as 0.00679 mm. E_f has been chosen as 54.2 GPa, from Table 5. G_m has been chosen as 1,287 MPa, taken from the literature [45]. ϕ_f has been calculated through *Eq. 6*, where the curaua fiber density (ρ_f) and PLA density (ρ_m) are 1.4 and 1.24 g/cm^3, respectively [23, 34]. m_f is the curaua fiber weight fraction.

$$\phi_f = \frac{m_f/\rho_f}{\frac{m_f}{\rho_f}+\frac{(1-m_f)}{\rho_m}} \quad (6)$$

Equation 5 considers the fiber–matrix adhesion to be satisfactory, without any uncoupling in the interphase. The l_c values obtained through *Eq. 5* are shown in Table 6. They have provided subsidies to the calculations of the Young's moduli by using Halpin–Tsai *Eqs. 2* and *3*. In addition, the experimentally measured l_f as average for each composite is also shown in Table 6.

As shown in Table 6, the necessary length of the curaua fibers to act as an effective reinforcement in the PLA matrix has to be above 0.098 mm for lower curaua fiber content and above 0.041 mm for higher fiber content. The length is inversely proportional to the fiber volume fraction. This has also been pointed out by Rosen [44].

The medium fiber length values stood greater than l_c for all six composite formulations. However, it was found that the higher the content of fibers is, the lower was their medium length, progressively approaching the respective l_c value. This indicates that the fiber breakage occurence increased for higher mass fraction of curaua during processing, and more fibers with lengths lower than l_c were seen. Fibers shorter than l_c do not efficiently reinforce the matrix, generally leading to lower mechanical properties overall.

Table 7 shows the calculated values of E_{cl}, Ect, and E_{random}, obtained using the real fiber lengths, and E obtained via tensile tests. It is observed that the measured E values were lower than those of E_{cl}, E_{ct}, and E_{random}. These results may be explained by some morphological aspects observed through the SEM, namely, partial fiber–matrix interface adhesion and presence of defects in this interface zone; deviating from ideality assumed in the adopted theoretical models. The calculated fiber length deviation (Table 6) points to an important observation, which is the relevance of the presence of fibers shorter than l_c. Those fibers contribute to the observed modulus values to be near the theoretical minimum limit. Nevertheless, as previously cited, the mechanical anchoring, good distribution/dispersion, and sufficient length of the fiber cells contributed to some mechanical properties such as impact resistance and Young's modulus when compared with the complete absence of fibers in the PLA.

CONCLUSIONS

Curaua leaf fibers have shown a satisfactory behavior as reinforcing fiber for PLA. The mixing torque is quite reasonable for PLA/curaua fiber composite prepared by an internal mixer. The curaua fiber stays thermally stable in the composites when processed in temperatures below 200°C. Curaua fiber significantly improves the PLA matrix crystallinity at lower fiber content.

The curaua fibers have shown that it is easy to filamentize them from the bundles when mixed with PLA by extrusion and molded by injection molding. Curaua single fibers were found well dispersed in the PLA matrix,

which may improve the stress transfer from the matrix to the reinforcing fibers.

Curaua fiber has improved the tensile modulus of the composites. It has also improved the impact strength for compositions up to 20% w/w. On the other hand, despite its high tensile strength compared with the PLA, it could not improve the composite tensile strength above the neat PLA.

It was possible to calculate tensile modulus for PLA/curaua fiber composites using different equations. Both superior and inferior moduli limits for the composites were established from the calculations. The experimental measured tensile modulus values became close to the inferior limit. Considering all experimental limitations, which may affect the assumed ideal hypothesis for the used equations, all the deviation observed from the theoretical calculated moduli were quite reasonable.

REFERENCES

1. A.K. Mohanty, M. Misra, and G. Hinrichsen, *Macromol. Mater. Eng.*, **276**, 1 (2000).
2. A.K. Mohanty, M. Misra, and L.T. Drzal, *J. Polym. Environ.*, **10**, 63 (2002).
3. M. Kolybaba, L.G. Tabil, S. Panigrahi, W.J. Crerar, T. Powell, and B. Wang, "Biodegradable Polymers: Past, Present and Future," in *CSAE/ASAE Annual Intersectional Meeting*, (2003).
4. W. Liu, M. Misra, P. Askeland, L.T. Drzal, and A.K. Mohanty, *Polymer*, **46**, 2710 (2005).
5. A.L. Leao, I.S. Machado, S.F. de Souza, and L. Soriano, *Acta Horticult.*, **822**, 227, (2009).
6. A.R. Sanadi, "Natural Fibers as Fillers/Reinforcements in Thermoplastics," in *Low Environmental Impact Polymers*, Rapra Technology Ltd., Shawbury (2004).
7. H. Zou, L. Wang, H. Gan, and C. Yi, *Polym. Compos.*, **33**, 1659 (2012).
8. A.K. Mohanty, M. Misra, and L.T. Drzal, *Compos. Interface*, **8**, 313 (2001).
9. A.R. Sanadi, D.F. Caulfield, R.E. Jacobson, and R.M. Rowell, *Ind. Eng. Chem. Res.*, **34**, 1889 (1995).
10. M.A. De Paoli, K.K.G. Fermoselli, M.A.S. Spinace, P.A. Santos, and J.C. Girioli, U.S. Patent 0,234,047 A1 (2009).
11. A.R. Sanadi, D.F. Caulfield, R.E. Jacobson, and R.M. Rowell, *Plast. Eng.*, **50**, 27 (1994).
12. R.A. Shanks, A. Hodzic, and D.J. Ridderhof, *J. Appl. Polym. Sci.*, **1**, 3620 (2006).
13. S.K. Chattopadhyay, R.K. Khandal, R. Uppaluri, and A.K. Ghoshal, *J. Appl. Polym. Sci.*, **113**, 3750 (2009).
14. D.E. Henton, P. Gruber, J. Lunt, and J. Randall, "Polylactic Acid Technology," in *Natural Fibers, Biopolymers, and Biocomposites*, Taylor & Francis, Boca Raton, FL (2005).
15. M.S. Huda, L.T. Drzal, M. Misra, and A.K. Mohanty, *J. Appl. Polym. Sci.*, **102**, 4856 (2006).
16. A.K. Bledzki, A. Jaszkiewicz, and D. Scherzer, *Compos. Part A*, **40**, 404 (2009).
17. A.M. Cunha, A.R. Campos, C. Cristovão, C. Vila, V. Santos, and J.C. Parajó, *Plast. Rubber Compos.*, **35**, 233 (2006).
18. B. Bax and J. Müssig, *Compos. Sci. Technol.*, **68**, 1601 (2008).
19. N.A. Ibrahim, W.M.Z.W. Yunus, M. Othman, K. Abdan, and K.A. Hadithon, *J. Reinf. Plast. Compos.*, **29**, 1099 (2010).
20. S.W. Lee and S. Wang, *Compos. Part A*, **37**, 80 (2006).
21. P.J. Jandas, S. Mohanty, and S.K. Nayak, *J. Polym. Environ.*, **20**, 583 (2012).
22. K. Oksman, M. Skrifvars, and J.F. Selin, *Compos. Sci. Technol.*, **63**, 1317 (2003).
23. K.G. Satyanarayana, J.L. Guimarães, and F. Wypych, *Compos. Part A*, **38**, 1694 (2007).
24. W.D. Callister Jr., *Fundamentals of Materials Science and Engineering: An Integrated Approach*, John Wiley & Sons, New York (2005).
25. S.N. Monteiro, R.C.M. Aquino, and F.P.D. Lopes, *J. Mater. Sci.*, **43**, 489 (2008).
26. H.S.P. Silva, H.L. Ornaghi Jr., J.H. Santos Almeida Jr., A.J. Zattera, and S.C. Amico, *Compos. Part A*, **38**, 1811 (2007).
27. L.V. Rossa, L.C. Scienza, and A.J. Zattera, *Polym. Compos.*, **34**, 450 (2013).
28. R. Zah, R. Hischier, A.L. Leao, and I. Braun, *J. Clean. Prod.*, **15**, 1032 (2007).
29. D.O. Castro, A. Ruvolo-Filho, and E. Frollini, *Polym. Test.*, **31**, 880 (2012).
30. F. Harnnecker, D.S. Rosa, and D.M. Lenz, *J. Polym. Environ.*, **20**, 237 (2012).
31. C. Borsoi, L.C. Scienza, and A.J. Zattera, *J. Appl. Polym. Sci.*, **128**, 653 (2012).
32. C. Borsoi, K.H. Berwig, L.C. Scienza, and A.J. Zattera, *Polym. Compos.*, **34**, 967 (2013).
33. M.A.S. Spinace, C.S. Lambert, K.K.G. Fermoselli, and M.A. De Paoli, *Carbohydr. Polym.*, **77**, 47 (2009).
34. Ingeo™, *Biopolymer 3251D Technical Data Sheet Injection Molding Process Guide*.
35. D. Garlotta, *J. Polym. Environ.*, **9**, 63 (2001).
36. B. Wunderlich, *Prog. Polym. Sci.*, **28**, 383 (2003).
37. M. Pyda, R.C. Bopp, and B. Wunderlich, *J. Chem. Thermodynamics*, **36**, 731 (2004).
38. N. Reddy and Y. Yang, *Trends Biotechnol.*, **23**, 22 (2005).
39. F. Tomczak, K.G. Satyanarayana, and T.H.D. Sydenstricker, *Compos. Part A*, **38**, 2227 (2007).
40. A.R. Sena Neto, M.A.M Araujo, F.V.D. Souza, L.H.C. Mattoso, and J.M. Marconcini, *Ind. Crops Prod.*, **43**, 529 (2013).
41. P.S. Mukherjee and K.G. Satyanarayana, *J. Mater. Sci.*, **21**, 51 (1986).
42. B.D. Agarwal, L.J. Broutman, and K. Chandrashekhara, *Analysis and Performance of Fiber Composites*, John Wiley & Sons, New York (2006).
43. K.K. Chawla, *Composite Material Science and Engineering*, Springer, New York (1998).
44. B.W. Rosen, "Mechanics of Composite Strengthening," in *Fiber Composite Materials*, American Society for Metals, Metals Park, OH (1965).
45. Moldflow Plastics Labs, *Moldflow Material Testing Report MAT2238 Nature Works PLA,* Cargill Dow LLC, Minnetonka, MN (2007).

 DOI 10.1002/pc